MOLECULAR AND CELLULAR BIOLOGY, Aug. 2005, p. 6603–6616 Vol. 25, No. 15
0270-7306/05/$08.00+0 doi:10.1128/MCB.25.15.6603–6616.2005

Mitochondrial Ribosomal Protein L41 Suppresses Cell Growth in Association with p53 and $p27^{Kip1}$

Young A Yoo,[1,2] Mi Jin Kim,[2,3] Jong Kuk Park,[1] Young Min Chung,[1] Jong Hyeok Lee,[1] Sung-Gil Chi,[2] Jun Suk Kim,[1,4]* and Young Do Yoo[3]*

Department of Internal Medicine and Division of Brain Korea 21 Program for Biomedical Science, Korea University College of Medicine, Seoul 136-705, South Korea[1]; School of Life Science and Biotechnology, Korea University, Seoul 136-705, South Korea[2]; Graduate School of Medicine, Korea University College of Medicine, Seoul 136-705, South Korea[3]; and Department of Internal Medicine, Korea University College of Medicine, Seoul 136-705, South Korea[4]

Received 18 November 2004/Returned for modification 5 January 2005/Accepted 11 May 2005

The p53 protein arrests the cell cycle at the G_1 phase when stabilized by the interaction between ribosomal proteins and HDM2 under growth-inhibitory conditions. Meanwhile, p53, when translocated to the mitochondria in response to cell death signals, induces apoptosis via transcription-independent mechanisms. In this report, we demonstrate that the mitochondrial ribosomal protein L41 (MRPL41) enhances p53 stability and contributes to p53-induced apoptosis in response to growth-inhibitory conditions such as actinomycin D treatment and serum starvation. An analysis of *MRPL41* expression in paired normal and tumor tissues revealed lower expression in tumor tissue. Ectopic *MRPL41* expression resulted in inhibition of the growth of cancer cells in tissue culture and tumor growth in nude mice. We discovered that MRPL41 protein is localized in the mitochondria, stabilizes the p53 protein, and enhances its translocation to the mitochondria, thereby inducing apoptosis. Interestingly, in the absence of p53, MRPL41 stabilizes the $p27^{Kip1}$ protein and arrests the cell cycle at the G_1 phase. These results suggest that MRPL41 plays an important role in p53-induced mitochondrion-dependent apoptosis and MRPL41 exerts a tumor-suppressive effect in association with p53 and $p27^{Kip1}$.

The tumor suppressor p53 is a key regulator of both the cell cycle and cell proliferation. The p53 protein is a potent transcription factor, which activates target genes and triggers growth arrest, DNA repair, or apoptosis in response to cellular genotoxic stresses (6, 11). The p53 protein has a short half-life, and its level is controlled mainly through its degradation by 26S proteasomes (14). p53 protein degradation is regulated largely by MDM2, which acts as the E3 ubiquitin ligase and targets p53 to the proteasome (8). The multiple-site phosphorylation of p53 abrogates the MDM2-mediated ubiquitination, resulting in the increased stability of p53.

Recent studies have demonstrated that p53 plays a role in the monitoring of the status of ribosomal biogenesis (18). Stresses on ribosomal biogenesis result in the arrest of cell growth or apoptosis to repair or remove the affected cells, probably via p53 activation. Several ribosomal proteins, including L5, L11, and L23, have been determined to activate p53 by inhibiting the MDM2/HDM2 (human homolog of MDM2)-mediated feedback regulation of p53 (1, 3, 4, 10, 12, 22). HDM2 interacts with the three ribosomal proteins through its different domains. This interaction inhibits HDM2-induced p53 polyubiquitination and degradation, leading to cell cycle arrest via p53 stabilization. Treatment with low concentrations of actinomycin D also causes an upshift in the interactions occurring between ribosomal proteins and HDM2. These studies suggest that ribosomal proteins play an important role in ribosomal biogenesis in response to some stresses.

Mitochondria act as a pivotal death regulator in response to DNA damage, growth factor withdrawal, hypoxia, and anticancer drug therapy (17). The exact mechanism underlying p53-mediated cell death in mitochondria after cellular stress has not yet been fully elucidated. However, several studies have reported that a fraction of activated wild-type p53 translocates directly to the mitochondrial surface of tumor cells in response to death signals, thus inducing transcription-independent p53-mediated cell death (2, 5, 13, 15, 16, 19). A variety of stress signals, including DNA damage and hypoxic stress, target p53 to the mitochondria in a wide spectrum of cell types.

Here, we report a gene, *MRPL41*, encoding the mitochondrial ribosomal protein, which was identified by differential-display PCR in the tumor tissues of a patient who was initially sensitive to chemotherapy but became resistant to chemotherapy after recurrence. The original purpose of the study was to obtain chemoresistance-related genes. Interestingly, we discovered that the *MRPL41* gene was located on chromosome 9q34.3, a region which frequently exhibits loss of heterozygosity in a wide range of tumors, including tumors associated with lung cancer (7, 9, 20, 21). Furthermore, *MRPL41* was either expressed at reduced levels or absent in most tumor types and cell lines. We attempted to ascertain whether MRPL41 inhibits the growth of cancer cells. We also attempted to evaluate the

* Corresponding author. Mailing address for Young Do Yoo: Graduate School of Medicine, Korea University College of Medicine, Anam Hospital, 126-1, 5ka, Anam-dong, Sungbuk-ku, Seoul 136-705, South Korea. Phone: 82-2-920-5762. Fax: 82-2-920-5762. E-mail: ydy1130@korea.ac.kr. Mailing address for Jun Suk Kim: Department of Internal Medicine, Korea University College of Medicine, Seoul 136-705, South Korea. Phone: 82-2-818-6651. Fax: 82-2-920-5762. E-mail: kjs6651@kumc.or.kr.

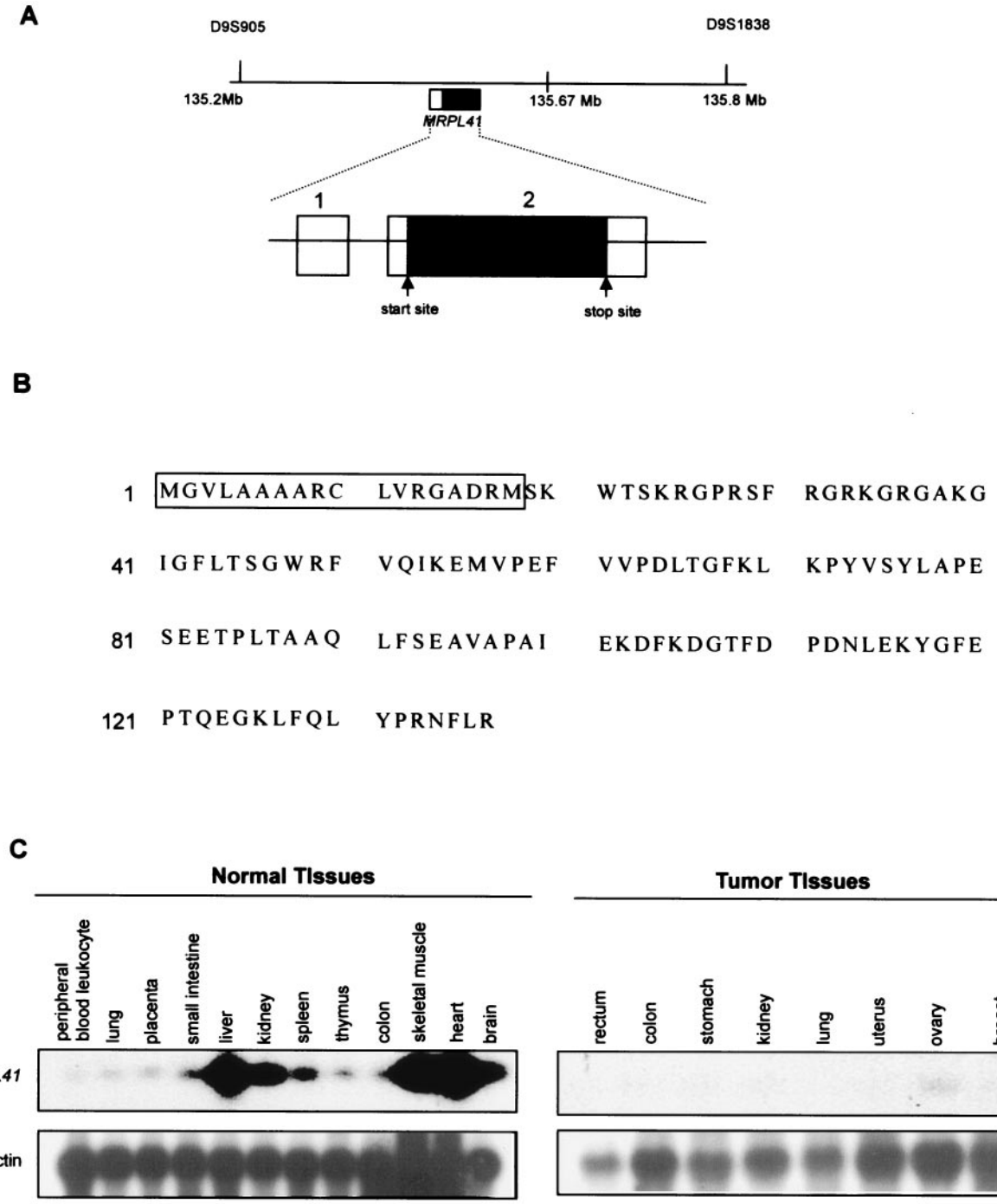

FIG. 1. *MRPL41* expression in various cells. (A) Physical and transcriptional mapping of the *MRPL41* gene. *MRPL41* is located within a 135-Mb region between the genetic markers D9S905 and D9S1838 on chromosome 9q34.3. Genetic markers are marked at the top. The intron-exon organization of the *MRPL41* gene is depicted as solid lines. The boxes represent two exons, and a black box represents the open reading frame. Vertical arrows under exon 2 indicate the predicted translational start and stop sites. (B) Amino acid sequence of the predicted protein encoded by *MRPL41*. The open box indicates the predicted mitochondrial leader sequence. (C) The analysis of *MRPL41* expression in human normal and tumor tissues. Northern blot analyses were performed to determine *MRPL41* expression in various normal and tumor tissues. Normal human 12-lane multiple tissue Northern blot (left panel) and human tumor MTN Northern blot (right panel) were hybridized with 146-bp ^{32}P-labeled HindIII fragments of *MRPL41* or a human β-*actin*-specific probe (Clontech). (D) Comparison of the expression of *MRPL41* in premalignant kidney cells and kidney tumor cells (left panel) and the expression of *MRPL41* in various cancer cell lines (right panel). Northern blot containing total RNA (10 μg) was performed with a 146-bp ^{32}P-labeled HindIII fragment of *MRPL41* and GAPDH probe. Cell lines are as follows: NCI-H211, small-cell lung cancer; SNU-638, gastric carcinoma; SW-620, colon cancer; MCF-7, breast carcinoma; HNSCC-PCI50, head and neck squamous cell carcinoma. (E) Comparison of the expression of *MRPL41* in non-small-cell lung cancer (NSCLC) cell lines and small-cell lung cancer (SCLC) cell lines. The 146-bp ^{32}P-labeled HindIII fragments of *MRPL41* and GAPDH probes were used. BEAS2B, premalignant lung cells.

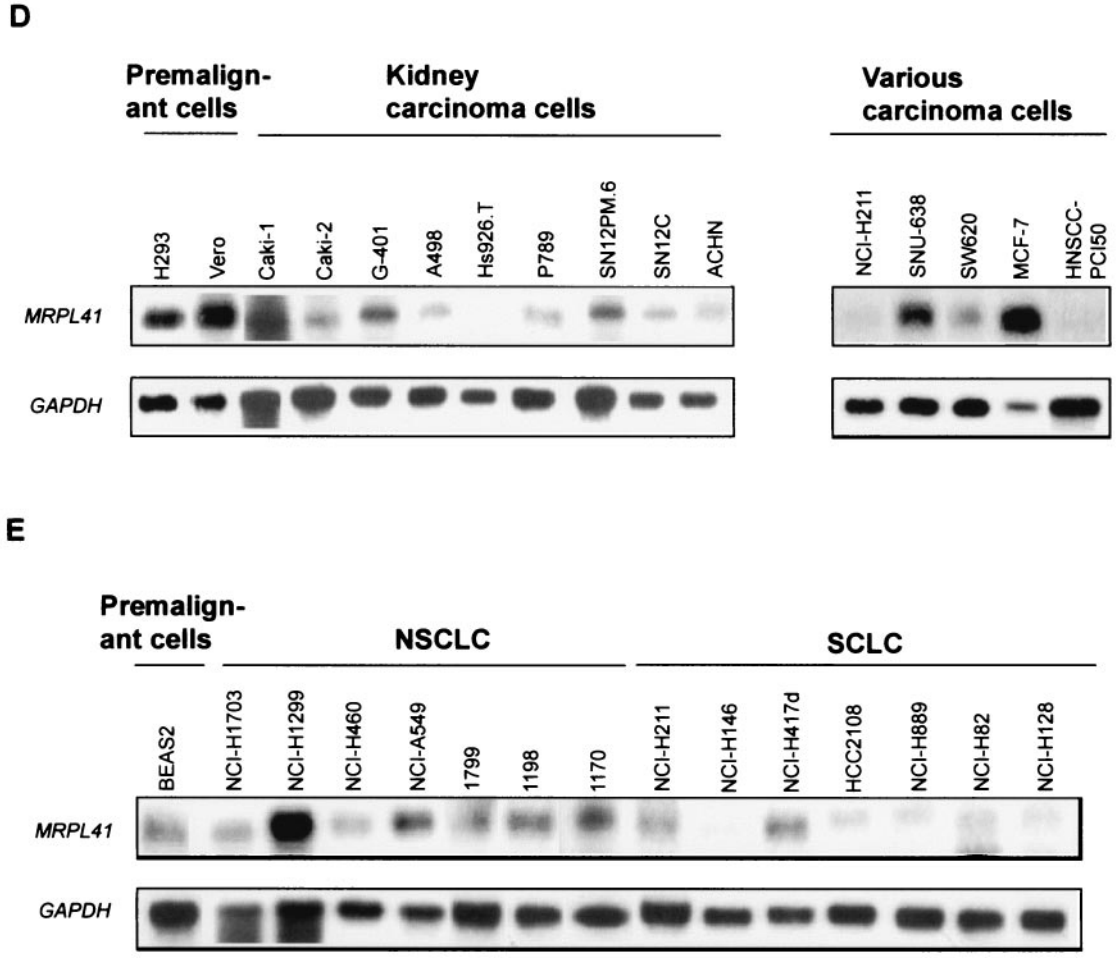

FIG. 1—*Continued*.

possible involvement of p53 with regard to MRPL41-induced growth suppression.

MATERIALS AND METHODS

Cell lines and tumor tissues. Cell lines used in these experiments were purchased from the American Type Culture Collection (ATCC; Manassas, VA). All cells were cultured according to ATCC's instructions. Tumor samples were derived from one patient with lymphoma undergoing surgical resection. Total RNA was isolated using Trizol reagent, according to the manufacturer's instructions (Life Technologies, Rockville, MD).

Differential-display PCR and cDNA library screening. Differential-display PCR was performed using the RNAimage mRNA differential-display system kit, according to the manufacturer's instructions (GeneHunter Co., Brookline, MA). The human lymph node cDNA library (Takara) was screened by plaque hybridization with an [α-^{32}P]dCTP-labeled partial 146-bp *MRPL41* cDNA probe digested with HindIII. [α-^{32}P]dCTP was obtained from Amersham Pharmacia, Inc.

Hybridization to expression arrays. The *MRPL41* cDNA or β-actin-specific probe provided with the blots was hybridized to normal human 12-lane multiple tissue, a human tumor MTN blot, and a human matched tumor/normal expression array (Clontech, Palo Alto, CA) following the manufacturer's instructions.

Northern blot analysis. Ten micrograms of total RNA was separated via 1% denaturing agarose gel electrophoresis and transferred to Nytran N nylon membranes (Schleicher & Schuell). The p53, p27, MRPL41, and GAPDH (glyceraldehyde-3-phosphate dehydrogenase) cDNA probes were labeled with a random-primed DNA labeling kit (Roche Molecular Biochemical, Indianapolis, IN). The random-primed ^{32}P-labeled *MRPL41* cDNA probe digested with HindIII was used for hybridization.

Vector construction and stable transfection. pcDNA3 and pcDNA3.1/myc-His were purchased from Invitrogen, and phrGFP-C was purchased from Stratagene. In order to generate the full-length cDNA encoding *MRPL41*, the full-length cDNA of *MRPL41* was subcloned into pcDNA3. To generate a Myc-tagged *MRPL41* or green fluorescent protein (GFP)-tagged *MRPL41*, PCR amplification of the *MRPL41* coding region was performed using the following primers: *MRPL41*-Forward, 5′-TAATACGACTCACTATAGGG-3′, and *MRPL41*-Reverse, 5′-ATCCGAGGCGCAGGAAGTTCCTGG-3′. The PCR product containing the entire *MRPL41* open reading frame was cloned into pGEM-T Easy (Promega, Madison, WI), and the insert was subcloned into either the pcDNA3.1/myc-His or phrGFP-C vector. Transfections were performed using Lipofectamine 2000 reagent (Invitrogen, Carlsbad, CA). After transfection of NCI-H211 cell lines with the respective plasmids, colonies were grown in culture medium supplemented with G418 (400 μg /ml) for 3 weeks. Discrete colonies were trypsinized in order to isolate stable *MRPL41*-transfected cells. *MRPL41* expression was confirmed by Northern blot analysis with an *MRPL41* cDNA probe. Ten clones were pooled in order to perform the colony formation assay and the cell cycle analysis.

Measurement of cell proliferation. The incorporation of 5-bromo-2′-deoxyuridine (BrdU) was utilized as the parameter by which DNA synthesis and cellular proliferation were measured. For BrdU incorporation, NCI-H211 stable transfectant cells were seeded at 4×10^3 cells in 100 μl culture medium per well in 96-well plates. After 4 days, BrdU labeling analysis was performed using a BrdU labeling and detection kit (Roche) according to the manufacturer's instructions.

Colony formation assay. ACHN cells (3×10^3) transiently transfected with *MRPL41* or control vector were seeded in a 100-mm dish and cultured in G418 (600 μg /ml)-supplemented medium (RPMI 1640 plus 10% fetal bovine serum). Fourteen to 21 days after seeding, G418-resistant colonies were counted via

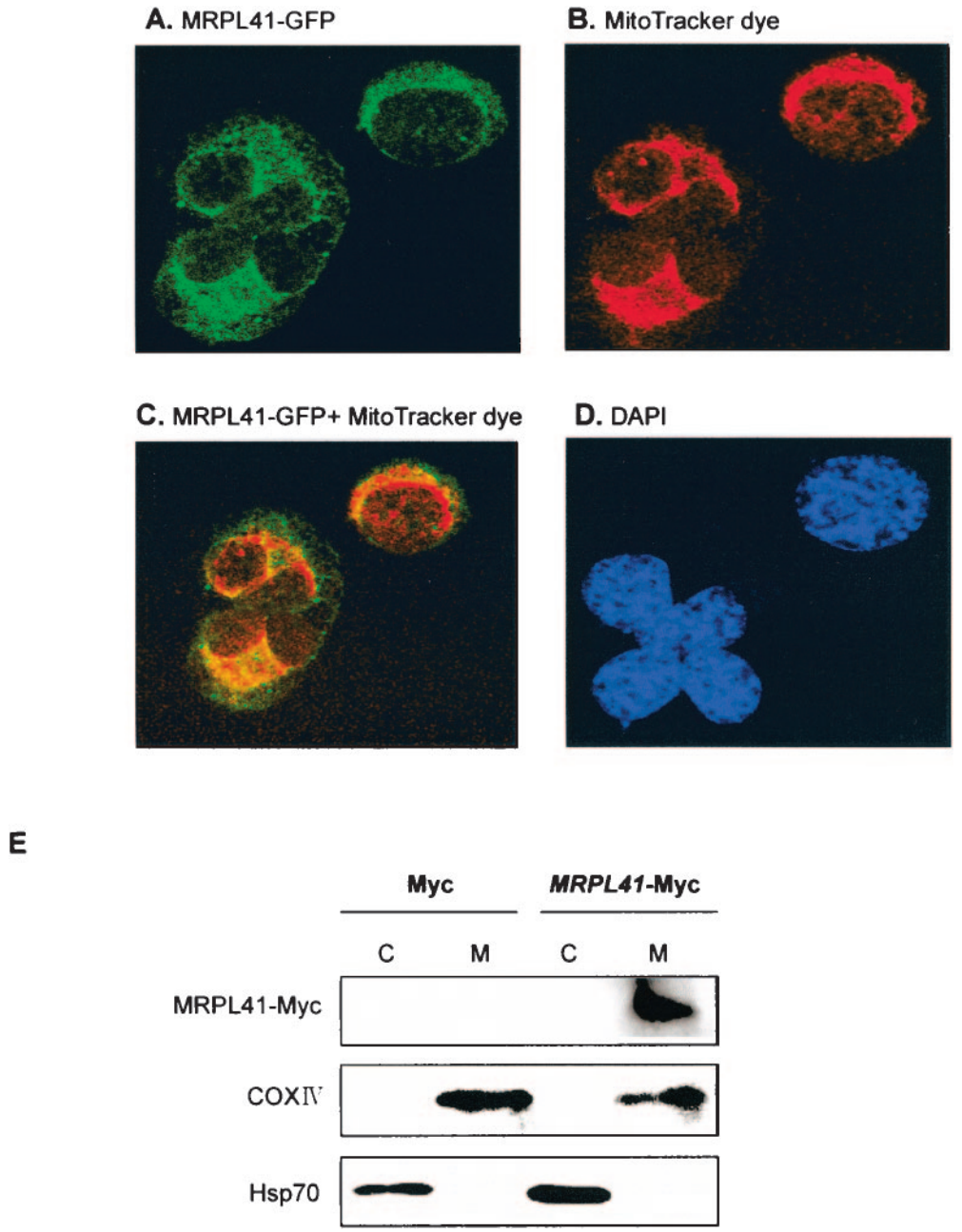

FIG. 2. The localization of MRPL41. H1299 cells were transfected with *MRPL41*-GFP or a control vector, fixed, and analyzed via confocal microscopy 48 h later. Mitochondria were stained with MitoTracker Red CMXRos dye. (A) GFP-tagged *MRPL41*-transfected cells. (B) Cells stained with MitoTracker Red dye. (C) Merged image demonstrating the colocalization of MRPL41 and mitochondria. (D) DAPI staining. (E) Western blot analysis with 10 μg mitochondrial and cytosolic extracts of NCI-H211 cells stably transfected with Myc-tagged *MRPL41* or the Myc control vector (pcDNA3.1/myc-His). Ten micrograms of the fraction was separated, transferred onto the membranes, and incubated with anti-Myc antibody. The membrane was then reblotted with either COXIV, the mitochondria marker (Clontech), or the cytoplasm marker anti-Hsp70 antibody. C, cytosolic fraction; M, mitochondrial fraction.

methylene blue dye staining. For the soft-agar growth assay, 5×10^3 NCI-H211 cells were mixed with 2 ml of medium (RPMI 1640 plus 10% fetal bovine serum) containing 0.25% agarose and seeded onto 3 ml 0.5% agarose in RPMI 1640 medium with 10% fetal calf serum in 60-mm dishes. After 6 weeks, cells were stained with nitroblue tetrazolium, according to the manufacturer's instructions (Sigma).

In vivo growth inhibition assay. We used 7-week-old, female BALB/c athymic nude mice (Charles River). Five animals per group were used. Cells (10^8) were injected into the trunk. Subsequently, tumor volume (short axis × short axis × long axis/2) was assessed every 3 days. Tumor tissues were removed 45 days after inoculation, and *MRPL41* expression was evaluated via Northern blot.

Cell cycle analysis. Cells stably transfected with *MRPL41* were seeded in 100-mm dishes. Forty-eight hours after seeding, cells were fixed with 70% ethanol for 2 h, washed with phosphate-buttered saline (PBS)-EDTA (5 mM), stained with 50 μg /ml of propidium iodide (Sigma) in PBS containing 20 μg /ml RNase A (Boehringer Mannheim), and incubated at 37°C for 1 h, and then DNA content was quantitated using the FACSCaliber system (Becton Dickinson). Ten thousand gated events per sample were acquired. The data were analyzed using

CellQuest software (Becton Dickinson). In order to conduct an analysis of the cell cycle in GFP-transfected cells, H1299 cells were transiently transfected with GFP-tagged *MRPL41* or GFP control vector. Forty-eight hours after transfection, flow cytometry analysis was performed, as described above. Cell cycle analysis of GFP-positive cells was carried out, as previously described elsewhere (23). For each analysis, 5,000 gated events of GFP-positive cells were collected.

Confocal microscopy. The entire coding region of *MRPL41* was generated by PCR, using the *MRPL41*-F and *MRPL41*-R primers, as described above. The PCR product was cloned into pGEM-T Easy (Promega), and the insert was subcloned into a phrGFP-C plasmid in order to construct the hybrid gene *MRPL41*-GFP fused with *MRPL41* at the N terminus of GFP. In order to evaluate the subcellular localization of MRPL41, ACHN cells were seeded on dishes containing 1-cm-diameter glass coverslips and transiently transfected with GFP-tagged *MRPL41* or a GFP control vector. Forty-eight hours later, cells were fixed in 3.7% paraformaldehyde for 10 min at 37°C, washed with PBS, and stained for 2.5 h with 100 nM MitoTracker Red CMXRos (Molecular Probes) or 2 μM 4′,6-diamidino-2-phenylindole (DAPI) fluorescence (Molecular Probes, Eugene, OR) at 37°C. The mitochondria and nuclei were visualized using a confocal microscope equipped with 506-nm and 600-nm laser beams.

In order to study the subcellular localization of exogenous p53, H1299 cells were cotransfected with p53 and GFP-tagged *MRPL41*. Twenty-four hours after transfection, cells were fixed by treatment with 3.7% paraformaldehyde, permeabilized with 0.5% Triton X-100 for 10 min, and blocked with 3% bovine serum albumin for 30 min at room temperature. After blocking, cells were incubated overnight at 4°C with polyclonal anti-p53 antibody (FL-393; Santa Cruz Biotechnology, Santa Cruz, CA), washed with PBS, and incubated for 30 min at room temperature with Alexa Fluor 590-labeled goat anti-rabbit immunoglobulin G (Molecular Probes). Following three washings with PBS, the slides were mounted with VECTASHIELD mounting medium (Vector Laboratories, Burlingame, CA). Immunofluorescence was detected via confocal microscopy (Bio-Rad MRC-1024/MP multiphoton microscope, using a multiline krypton/argon laser for standard confocal microscopy, interfaced with a Zeiss Axiovert microscope).

Production of anti-MRPL41 polyclonal antibody. We purchased anti-MRPL41 antibody produced by Aprogen (Daejon, South Korea). Briefly, a peptide (KWTSKRGPRSFRGRKGRGAKGC) was synthesized and 20 μg of the peptide was injected subcutaneously into a mouse. Whole blood was collected after boosting four times.

Western blot and CHX treatment. NCI-H211, 293, and H1299 cells were transfected with plasmids, as indicated in the figure legends, and were lysed with radioimmunoprecipitation assay buffer (50 mM Tris, 150 mM NaCl, 1% Triton X-100, 0.1% sodium dodecyl sulfate [SDS], 1% Na deoxycholate [pH 7.4]) supplemented with protease inhibitors (1 mM phenylmethylsulfonyl fluoride, 10 μg/ml pepstatin A, 10 μg/ml aprotinin, and 5 μg/ml leupeptin). Protein concentrations were measured using the Bio-Rad (Hercules, CA) protein assay kit. Protein lysates were resolved by SDS-polyacrylamide gel electrophoresis (PAGE) and then transferred onto nitrocellulose membranes (Hybond-P; Amersham Biosciences, Piscataway, NJ), blocked by PBS containing 0.2% Tween 20 and 5% nonfat dry milk, and incubated with primary antibody and with horseradish peroxidase-labeled secondary antibody. The signal was exposed on X-ray film. The antibody used was monoclonal anti-p53 antibody (DO-1; Santa Cruz Biotechnology), polyclonal anti-p27 antibody (BD Transduction Laboratories, San Diego, CA), monoclonal anti-MDM2 antibody (Ab-2; Oncogene Research Products, San Diego, CA), monoclonal anti-Myc antibody (R950-25; Invitrogen), and monoclonal anti-β-actin antibody (AC-74; Sigma). For cycloheximide (CHX; Sigma) treatment, NIC-H211 cells stably transfected with MRPL41 or control vector were treated with 50μg/ml cycloheximide. In NCI-H1299 cells, 48 h after transfection with either p53 alone or with *MRPL41*-Myc, the medium was supplemented with 50μg/ml of cycloheximide. The cells were then collected at the indicated time points.

Fractionation of mitochondria. NCI-H211 or H1299 cells either stably or transiently transfected with the *MRPL41*-Myc or Myc control were collected from six 150-mm plates, and mitochondrial fractions were isolated according to the manufacturer's instructions (Apo Alert mitochondrial fractionation kit; Clontech). For Western blot analysis, 10 μg of protein per fraction was loaded and incubated with anti-p53, anti-COXIV (Clontech), anti-Hsp70 (K-20; Santa Cruz Biotechnology), and anti-cytochrome *c* antibody (Clontech).

In vivo ubiquitination assay. The H1299 cells were cotransfected with 0.1 μg of p53 or an increasing amount of *MRPL41*-Myc (0.3 μg and 1 μg). At 24 h after transfection, cells were treated with proteosomal inhibitor MG-132 (10 μM) (Calbiochem) and incubated for 6 h. The cells were then lysed with radioimmunoprecipitation assay buffer supplemented with protease inhibitors. The cell extracts were immunoprecipitated with 1 μg of anti-p53 antibody and subsequently resolved by 4 to 20% gradient SDS-polyacrylamide gel electrophoresis. The ubiquitinated p53s were analyzed by Western blotting with monoclonal anti-Ub antibody (Sigma; P4D1).

RNAi transfection. The stealth RNA interference (RNAi) duplex targeting nucleotides 417 to 441 relative to the translation stop codon of MRPL41 mRNA or fluorescence-labeled double-stranded RNA (dsRNA) oligomer (BLOCK iT fluorescence oligonucleotide) as a control were synthesized at Invitrogen. The stealth RNAi sequences of the MRPL41 were 5′-ACCUUCGACCCUGACAA CCUGGAAA-3′ and 5′-UUUCCAGGUUGUCAGGGUCGAAGU-3′. Cells were transfected with 100 nM MRPL41 RNAi duplex or control dsRNA using Lipofectamine 2000 reagent according to the manufacturer's instructions. p27 small interfering RNA (siRNA) was purchased from Santa Cruz.

RESULTS

Identification and expression of *MRPL41*. In order to identify the genes expressed differentially in tumor tissue, we performed differential-display PCR and identified the 136-bp partial *MRPL41* cDNA fragment which had been down-regulated in the tumor tissue. Using human lymph node cDNA library screening, we cloned full-length *MRPL41* cDNA, which consists of two exons and encodes a 137-amino-acid peptide (Fig. 1A). The MRPL41 protein contains an 18-amino-acid mitochondrial targeting sequence (Fig. 1B).

In order to assess *MRPL41* expression in various normal and tumor tissues, the *MRPL41* cDNA fragment was hybridized to mRNA and cDNA samples derived from a variety of human normal and tumor tissues. Northern blot analysis revealed an *MRPL41* transcript approximately 600 bp in length. The expression of this gene was detected in diverse normal tissues but not in tumor tissues (Fig. 1C). *MRPL41* expression was also assessed in a panel of kidney cells, two premalignant kidney cell lines, and nine kidney carcinoma cell lines (Fig. 1D). *MRPL41* expression in most kidney carcinoma cell lines was found to be lower than in premalignant kidney cell lines (67%, 6/9). We also assessed *MRPL41* expression in other tumor cell lines, via the application of the same *MRPL41* DNA fragment (Fig. 1D and E). Our results indicated that *MRPL41* expression was lower in most small-cell lung cancer cell lines than in non-small-cell lung cancer cell lines (86%, 6/7). This suggests that *MRPL41* expression may be down-regulated during tumorigenesis and that this decreased MRPL41 activity may contribute to tumor progression in both the kidney and the lung.

The localization of MRPL41. In order to determine the localization of MRPL41, the hybrid gene *MRPL41* tagged with green fluorescent protein (*MRPL41*-GFP) was introduced to H1299 cells. The MRPL41 protein was detected in the mitochondrial position as dotted patterns (Fig. 2A). The transfectants were stained with the mitochondrion-specific dye MitoTracker and analyzed with a confocal microscope (Fig. 2B). The MitoTracker red fluorescent dye completely overlapped the green MRPL41-GFP signals (Fig. 2C). This demonstrates that the MRPL41 protein is localized in the mitochondria. This is consistent with our prediction (based on sequence analysis) that MRPL41 is expressed in the mitochondria.

In order to confirm that the MRPL41 protein is localized in the mitochondria, the mitochondrial fractional experiment was performed with NCI-H211 cells stably transfected with the hybrid Myc gene tagged to *MRPL41* (*MRPL41*-Myc). Control cells were transfected with the Myc vector. As expected, MRPL41 protein was detected in the purified mitochondrial fraction of NCI-H211 cells which were stably transfected with

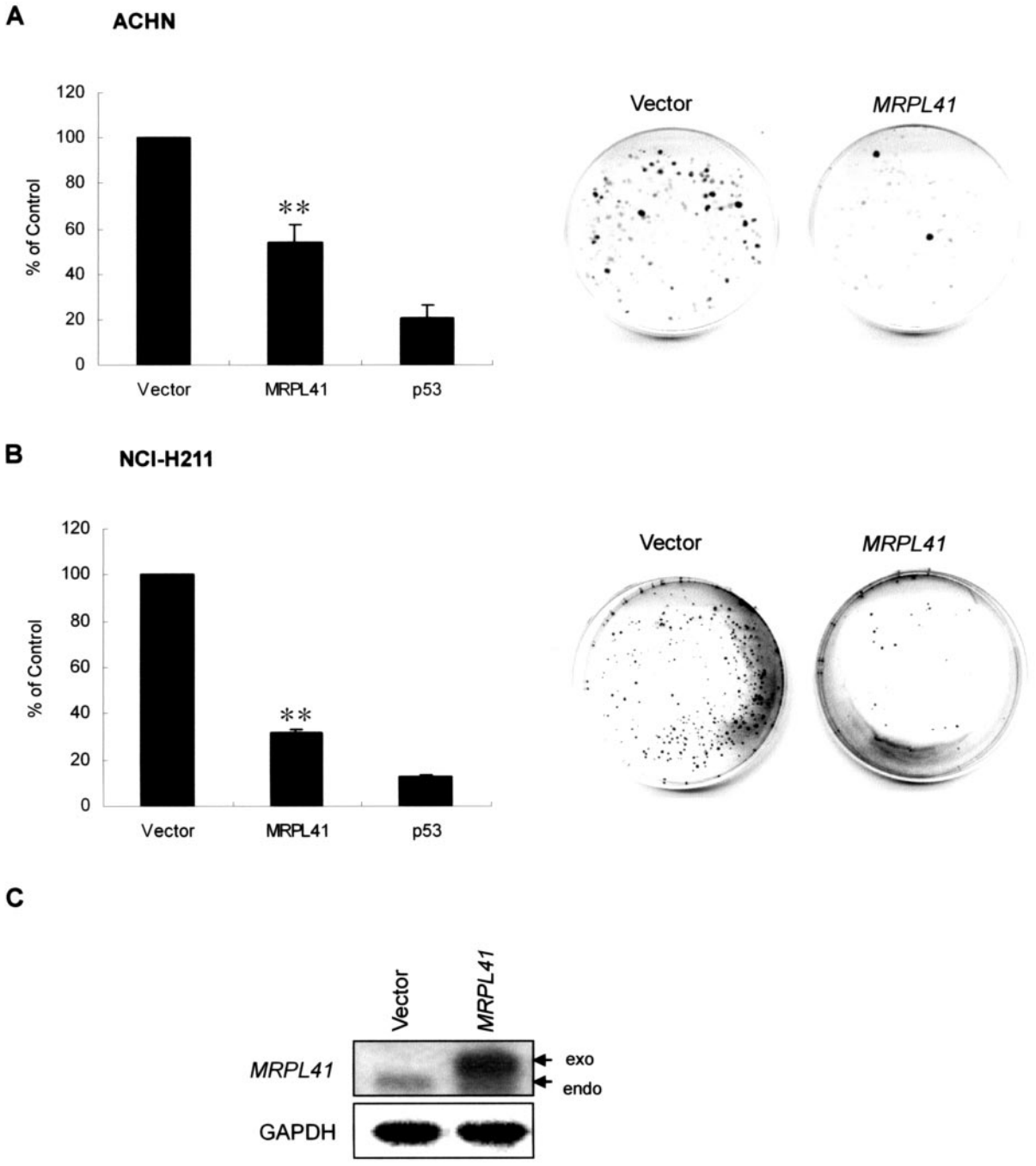

FIG. 3. Growth inhibition of tumor cells by MRPL41 in vitro and in vivo. (A) The enumeration of ACHN colonies. ACHN cells were transfected with *MRPL41*, cultured in suspension with G418, and stained with methylene blue, and colonies were counted. Double asterisk, $P < 0.001$ versus the vector (Student's *t* test). (B) NCI-H211 cells were transfected with *MRPL41*, cultured in soft agar with G418, and stained with nitroblue tetrazolium, and colonies were counted. The data are expressed as the means ± standard deviations (SD) from three independent experiments. Vector, pcDNA3; *MRPL41*-S, pcDNA3-*MRPL41*. (C) Northern blot of NCI-H211. The ectopic expression of *MRPL41* in stable transfectant cells was confirmed by Northern blotting. The expression levels of endogenous (endo) and exogenous (exo) *MRPL41* are shown. (D) The enumeration of NCI-H211 colonies. NCI-H211 cells were stably transfected with *MRPL41* or control vector, cultured for 5 weeks in soft agar in the presence of G418, and stained with nitroblue tetrazolium, and colonies were counted. The data represent the means of three independent experiments ± SD. (E) The BrdU labeling assay. NCI-H211 cells stably transfected with *MRPL41* or control vector were labeled with BrdU as described in Materials and Methods. Incorporated BrdU was measured by reading optical densities at 405 nm against the reference of 490 nm. The results are presented as the means of three independent experiments ± SD. (F) The effect of *MRPL41* on the formation of tumors in vivo. Five animals were injected with NCI-H211 cells stably transfected with *MRPL41* or control vector, as described in Materials and Methods. Tumors were measured every 3 days for 45 days. The data are expressed as the means of three independent experiments ± SD. Asterisk, $P < 0.05$ versus the vector (Student's *t* test). (G) The expression of introduced *MRPL41* in nude mice was confirmed via Northern blot.

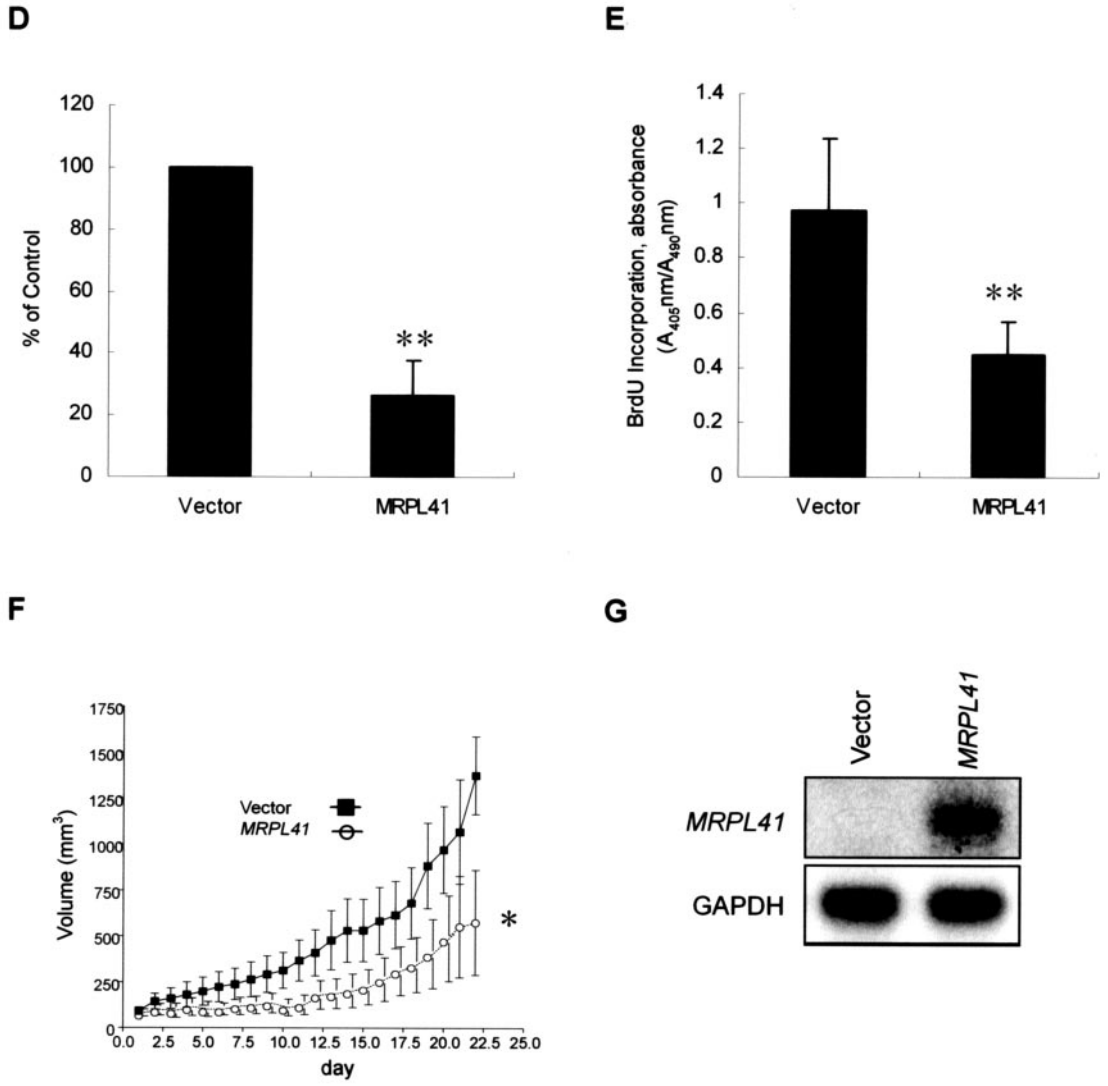

FIG. 3—*Continued*.

MRPL41-Myc (Fig. 2E). This was clearly not due to the contamination of the cytosolic fraction, as the marker of the cytosolic fraction Hsp 70 was not detected in the mitochondrial fraction (Fig. 2E).

MRPL41 suppresses tumor cell growth. To determine whether *MRPL41* inhibits the growth of tumor cells expressing low levels of *MRPL41* mRNA, we performed colony formation assays. Transient transfection of ACHN kidney carcinoma cells with *MRPL41* inhibited growth by 45.7% (Fig. 3A). In the experiments, negative control cells were transfected solely with vectors. Positive control cells were transfected with wild-type p53, which has been demonstrated to inhibit tumor cell growth (4).

We also investigated MRPL41's effects on the ability of NCI-H211 cells (small-cell lung cancer) to form colonies in an anchorage-independent manner. NCI-H211 cells transfected with *MRPL41* or control vector were cultured in soft agar containing G418. Three weeks later, the colonies were counted. As shown in Fig. 3B, the reintroduction of *MRPL41* inhibited the growth of NCI-H211 cells by 68%. We constructed NCI-H211 cells which stably expressed *MRPL41* and assessed its expression (Fig 3C). The number of NCI-H211 cell colonies overexpressing *MRPL41* was 73.6% lower than that for the control cells (Fig. 3D). In order to verify the MRPL41-induced inhibition of cell growth, we performed BrdU labeling assays. As we had observed in the colony formation assay, the proliferation rate of NCI-H211 cells overexpressing *MRPL41* was 54.1% lower than that for the control cells (Fig. 3E).

In addition, we examined *MRPL41*'s effects on cell proliferation in vivo. NCI-H211 cells stably transfected with *MRPL41* were subcutaneously injected into BALB/c athymic nude mice. Tumor formation was detected beginning 7 days after injection. In animals treated with NCI-H211 cells stably expressing *MRPL41*, tumor formation was substantially delayed (Fig. 3F). Figure 3G shows the expression of exogenously introduced *MRPL41* in tumor transplants. These results suggest that MRPL41 inhibits the growth of tumor cells under both in vitro and in vivo conditions.

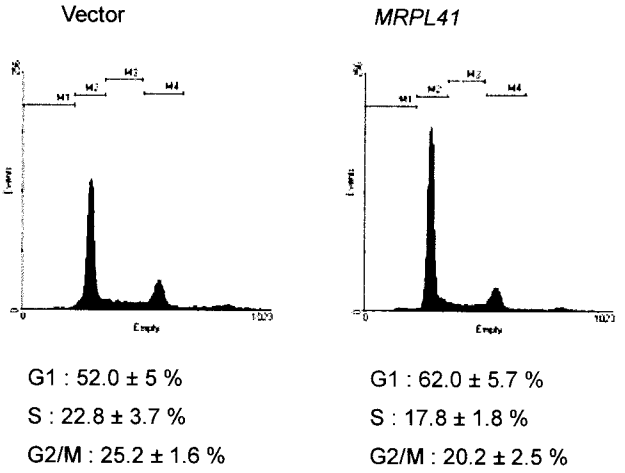

FIG. 4. MRPL41-induced cell cycle arrest at G_1. Flow cytometry of NCI-H211 stably transfected with *MRPL41* or control vector. Cells were harvested, stained with propidium iodide, and analyzed by FACScan flow cytometry. Over 10,000 cells were acquired for analysis. The data are expressed as the means of three independent experiments ± standard deviations.

MRPL41 arrests the cell cycle at the G_1 phase. In order to determine whether MRPL41 regulates cell cycle progression, the DNA content of cells stably transfected with *MRPL41* was analyzed via flow-cytometric analysis. Figure 4 shows that NCI-H211 cells expressing *MRPL41* were arrested in the G_1 phase of the cell cycle. The fraction in the G_1 phase increased from 52% to 62%. This indicates that MRPL41 inhibits small-cell lung cancer cell proliferation by arresting the cell cycle at the G_1 phase.

In order to ascertain the mechanism underlying the MRPL41-mediated arrest of the cell cycle, we examined the cell cycle regulator induced by MRPL41. p53 expression was found to be elevated in NCI-H211 cells stably transfected with *MRPL41*-Myc (Fig. 5A). However, MRPL41 had no effect on the expression of MDM2, a negative regulator of p53. To verify the induction of p53 by MRPL41, NCI-H211 and HEK 293T cells were transiently transfected with increasing amounts of *MRPL41*-Myc and then levels of p53 expression were assessed. Endogenous p53 levels increased significantly in both cell lines transfected with *MRPL41*-Myc, in which *MRPL41* expression was evaluated using anti-Myc antibody (Fig. 5B and C). As the level of p53 protein can be affected by either its stability or the transcriptional regulation of the p53 gene, we attempted to determine whether MRPL41 increases p53 expression by enhancing its transcription. The transcription level of p53 mRNA in cells stably transfected with *MRPL41* was found to be comparable to control cells (Fig. 5D). In the *MRPL41* transfectants, the p53 expression was enhanced, but not transcription. Therefore, in order to determine whether MRPL41 enhances the stability of p53, the p53-null lung cancer H1299 cells were transfected with either p53 alone or with *MRPL41*-Myc. As expected, the stability of the p53 protein in the H1299 cells cotransfected with p53 and *MRPL41* was higher than in the cells transfected with p53 alone (Fig. 5E). To further verify that MRPL41 stabilizes p53, NCI-H211 cells stably transfected with *MRPL41* or control vector were treated with cycloheximide, a translation inhibitor. NCI-H1299 cells were transfected with either p53 alone or with *MRPL41* and were then treated with cycloheximide. Two hours after this procedure, p53 protein could no longer be detected in the control cells. However, no remarkable decrease in the amount of p53 protein was observed in either of the cell lines transfected with *MRPL41* (Fig. 5F). To identify the mechanism by which MRPL41 induces p53 stabilization, an in vivo ubiquitination assay was performed. As shown in Fig. 5G, MRPL41 inhibits p53 ubiquitination. The data suggest that MRPL41 regulates p53 expression at the posttranslational level.

Since the cell cycle arrest at the G_1 phase is influenced by Cdk inhibitors, we examined the expression of $p27^{Kip1}$ and $p21^{Waf1/CIP1}$ in NCI-H211 cells stably transfected with *MRPL41*. $p27^{Kip1}$ expression was found to be elevated in cells stably or transiently transfected with *MRPL41* (Fig. 6A and B). However, there were no alterations observed in the amount of $p21^{Waf1/CIP1}$ in the NCI-H211 cells (data not shown). In Fig. 4, we showed that increased expression of MRPL41 induced cell cycle arrest at the G_1 phase. To examine whether the p53 protein, found in high levels in NCI-H211 cells, is transcriptionally active and, therefore, induces cell cycle arrest, Northern blot analysis for p21 and HDM2 was performed in NCI-H211 cells expressing MRPL41. Even though MRPL41 enhanced the amount of the p53 protein in NCI-H211 cells, increased p21 and HDM2 mRNA levels in NCI-H211 cells expressing MRPL41 were not induced (data not shown). This result demonstrated that p53, induced by MRPL41 in NCI-H211 cells, is transcriptionally inactive. As the ectopic expression of MRPL41 caused increased p53 expression at the posttranslational level, we attempted to determine whether the induction of $p27^{Kip1}$ by MRPL41 was a p53-dependent process. We transfected p53-null H1299 cells with increasing amounts of *MRPL41*, and then $p27^{Kip1}$ expression was examined via Western blot. As shown in Fig. 6C, MRPL41 caused an accumulation of $p27^{Kip1}$, even in the absence of p53. As MRPL41 promoted the levels of p53 by increasing its half-life, we assumed that MRPL41 might, similarly, increase the half-life of $p27^{Kip1}$. Indeed, the overexpression of MRPL41 in NCI-H211 cells stably transfected with *MRPL41* had no effect on the transcription level of $p27^{Kip1}$ mRNA (Fig. 6D). The stability of $p27^{Kip1}$ in the H1299 cells transfected with *MRPL41* also increased after treatment with cycloheximide (Fig. 6E). This demonstrates that MRPL41 also exerts a stabilizing effect on $p27^{Kip1}$. In order to determine whether the increased level of $p27^{Kip1}$ induced by MRPL41 affected cell cycle progression in the H1299 cells, the DNA content of the H1299 cells transiently transfected with GFP-tagged *MRPL41* was quantified via flow-cytometric analysis. As shown in Fig. 6F, H1299 cells expressing *MRPL41* were arrested in the G_1 phase of the cell cycle, compared to the GFP-expressing cells. To observe whether the real reason for G_1 arrest is $p27^{Kip1}$ induction, $p27^{Kip1}$ siRNA was transiently transfected into NCI-H211 cells stably expressing MRPL41. Transient transfection of $p27^{Kip1}$ siRNA efficiently down-regulated $p27^{Kip1}$ expression (Fig. 6G). We then examined whether the siRNA-mediated blocking of $p27^{Kip1}$ expression could release this cell cycle arrest at the G_1 phase. As shown in Fig. 6H, flow-cytometric analysis showed that MRPL41 expression induced cell cycle arrest at the G_1 phase and that $p27^{Kip1}$ siRNA treatment released cells from

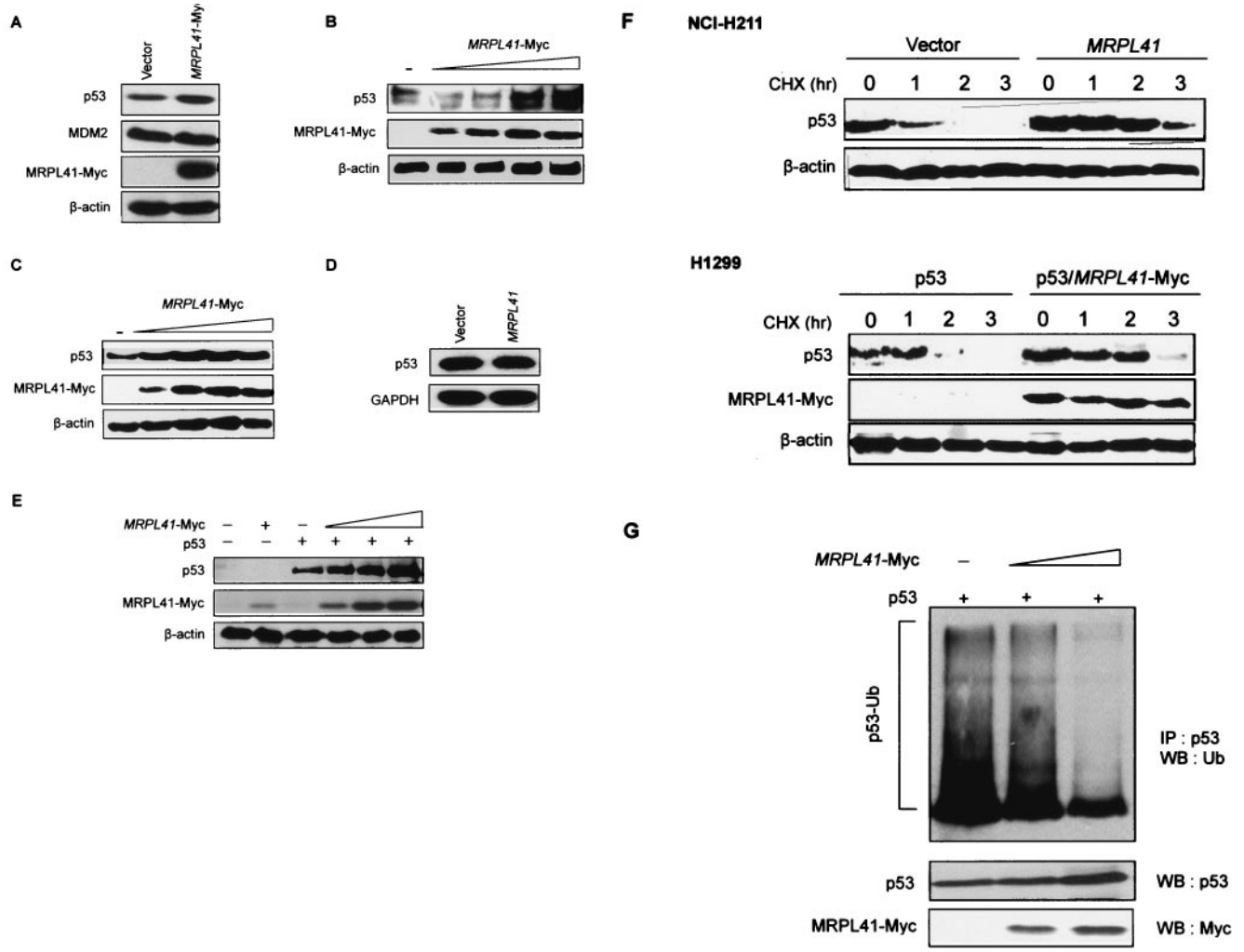

FIG. 5. MRPL41 stabilized p53. (A) Western blot analysis. Forty micrograms of cell lysates of NCI-H211 cells stably transfected with *MRPL41*-Myc or control vector was resolved via SDS-PAGE, and Western blotting with anti-p53, anti-MDM2, or anti-β-actin antibodies was carried out. Increasing amounts of *MRPL41*-Myc (0.1 μg, 0.3 μg, 0.5 μg, and 1 μg) were transfected into NCI-H211 (B) and HEK-293T cells (C), and Western blotting with anti-p53, anti-Myc, or anti-β-actin antibodies was carried out. (D) Northern blot analysis of p53 in stable transfectant NCI-H211 cells. (E) Western blot analysis of NCI-H1299 cells cotransfected with equal amounts of p53 and increasing amounts of *MRPL41*-Myc. The lysates of cells cotransfected with 0.1 μg of p53 or increasing amounts of *MRPL41*-Myc (0.1 μg, 0.3 μg, 0.5 μg, and 1 μg) were resolved by SDS-PAGE and stained with anti-p53, anti-Myc, or anti-β-actin antibodies. (F) Effect of cycloheximide on p53-protein stability. NCI-H211 cells stably transfected with *MRPL41* or control vector were treated with cycloheximide (50 μg/ml). In NCI-H1299 cells, cells were transfected either with p53 alone or with *MRPL41* and treated with cycloheximide 48 h later. Extracts were subjected to SDS-PAGE, and p53 stability was evaluated via Western blot with anti-p53 antibody. (G) In vivo ubiquitination assay. H1299 cells were transfected with 0.1 μg of p53 and increasing amounts of *MRPL41*-Myc (0.3 μg and 1 μg). After 24 h, 10 μM of MG132 was treated for 6 h and then harvested. The lysates of cells were immunoprecipitated with anti-p53 antibody, followed by Western blot by anti-Ub antibody.

MRPL41-induced cell cycle arrest. These results demonstrate that MRPL41 exerts a stabilizing effect on $p27^{Kip1}$ protein and arrests the cell cycle at the G_1 phase.

MRPL41 triggers p53-induced mitochondrion-dependent apoptosis. Recently, several groups reported that a fraction of wild-type p53 translocated to the mitochondrial membrane of cultured tumor cells under stress conditions, there promoting apoptosis (2, 5, 13, 15, 16, 19). Our data indicated that the MRPL41 protein is localized in the mitochondria (Fig. 2), accumulates $p27^{Kip1}$ protein, and induces cell cycle arrest at the G_1 phase in the absence of p53 (Fig. 6). Next, we attempted to discover whether MRPL41 induced apoptosis in H1299 cells cotransfected with p53 and *MRPL41*-GFP. As expected, the growth of both the cells transfected with *MRPL41*-GFP alone and the cells transfected with low levels of p53 (0.1 μg) were arrested in the G_1 phase, whereas the cells which were cotransfected with *MRPL41*-GFP and p53 exhibited significant apoptosis (Fig. 7A). The sub-G_1 population in the p53-MRPL41-expressing cells increased to 20.3%. The release of cytochrome *c* into the cytoplasm constitutes a critical step in the mitochondrial apoptotic pathway. Thus, in order to corroborate the above results, we attempted to discern whether MRPL41 induced the translocation of cytochrome *c* into the cytoplasm in H1299 cells cotransfected with *MRPL41*-Myc and p53. As

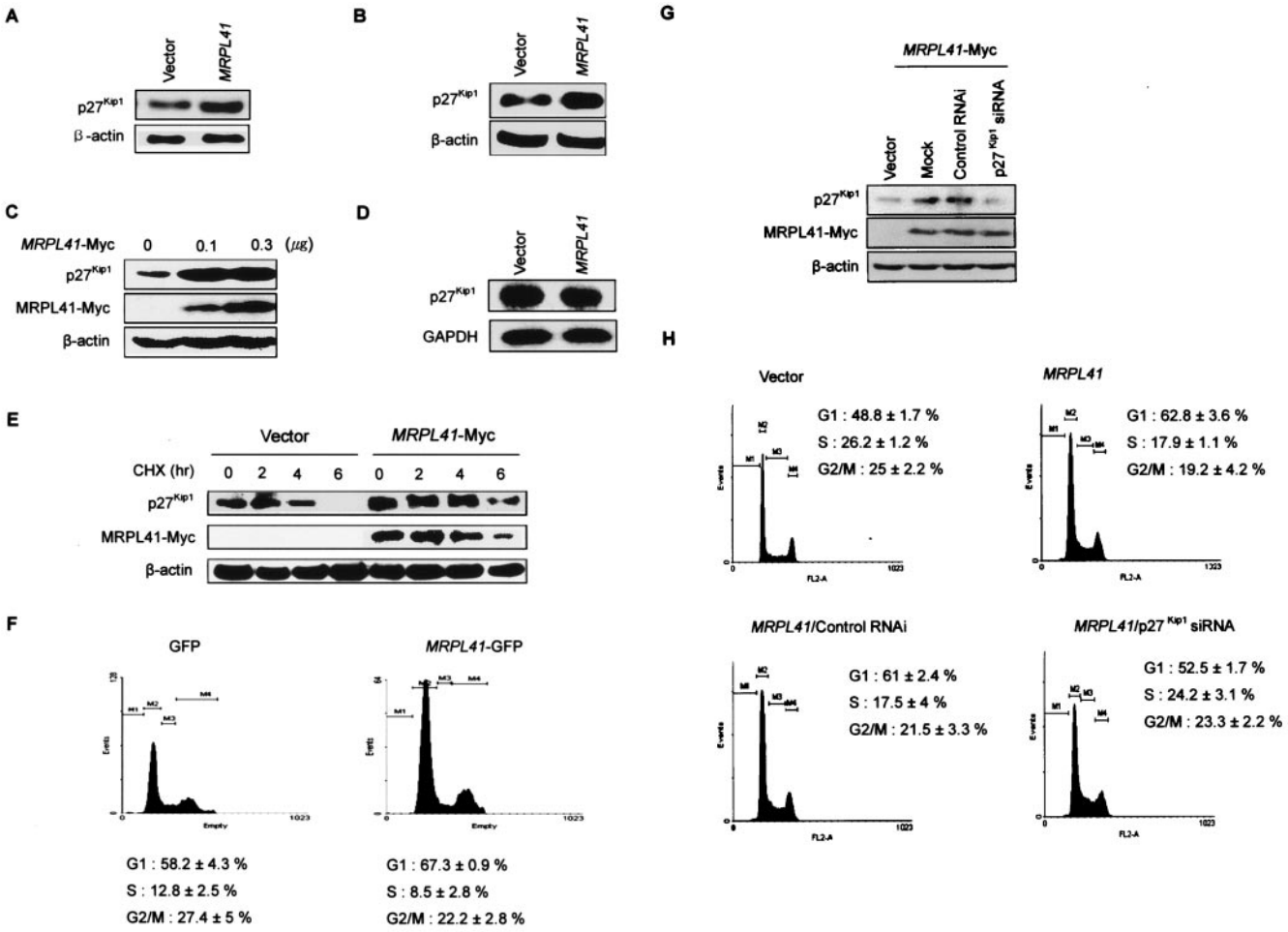

FIG. 6. MRPL41 stabilized $p27^{Kip1}$ and induced cell cycle arrest at the G_1 phase in the p53-null NCI-H1299 cells. (A) Western blot analysis. Forty micrograms of cell lysates of NCI-H211 cells stably transfected with *MRPL41* or control vector was resolved by SDS-PAGE, and Western blotting with anti-p27 ^{Kip1} or anti-β-actin antibodies was carried out. (B) Forty micrograms of cell lysate of NCI-H211 cells transiently transfected with *MRPL41* or control vector was resolved by SDS-PAGE, and Western blotting with anti-p27 ^{Kip1} or anti-β-actin antibodies was performed. (C) Forty micrograms of cell lysates of NCI-H1299 cells transiently transfected with *MRPL41* or control vector was resolved by SDS-PAGE, and Western blotting with anti-$p27^{Kip1}$, anti-Myc, or anti-β-actin antibodies was performed. (D) Northern blot analysis of p27 ^{Kip1} in stable transfectant NCI-H211 cells. (E) Effects of cycloheximide on p27 ^{Kip1} protein stability. NCI-H1299 cells were transfected with p53 alone or with *MRPL41* and then treated with cycloheximide 48 h later. Extracts were subjected to SDS-PAGE, and p27 ^{Kip1} stability was assessed by Western blotting with anti-p27 ^{Kip1} antibody. (F) NCI-H1299 cells were transfected with GFP or GFP-tagged *MRPL41* and stained with propidium iodide 48 h later. The DNA content of GFP-expressing cells was quantitated by two-color fluorescence-activated cell sorting. Over 5,000 cells were used for this analysis. (G) One hundred nanomolar of $p27^{Kip1}$ siRNA or a control RNA duplex was transiently transfected into NCI-H211 cells expressing MRPL41 for 24 h. After 24 h, 40 μg cell lysates was resolved by SDS-PAGE, and Western blotting with anti-$p27^{Kip1}$, anti-Myc, or anti-β-actin antibodies was performed. (H) For flow-cytometric analysis, cells were harvested, stained with propidium iodide, and analyzed by FACScan flow cytometry. Over 10,000 cells were acquired for analysis.

shown in Fig. 7B, H1299 cells cotransfected with *MRPL41*-Myc and p53 exhibited significantly higher cytochrome *c* release into the cytoplasm than did the cells transfected solely with p53. These observations imply that MRPL41 induced apoptosis via the stabilization of p53 and the induction of p53 translocation to the mitochondria. However, MRPL41 was also found to induce G_1 arrest via the stabilization of $p27^{Kip1}$ in the absence of p53.

As shown in Fig. 7B, p53 was detected in both mitochondrial and cytosolic fractions in the H1299 cells cotransfected with *MRPL41*-Myc and p53. Next, we further determined whether increased MRPL41 expression induced p53 translocation into the mitochondria. In order to determine whether the increasing amount of p53 stabilized by MRPL41 triggered mitochondrial p53 translocation, the p53 levels were augmented by cotransfection with equal amounts of p53 and increasing amounts of MRPL41 and the nuclear export of p53 was examined via confocal microscopy. As shown in Fig. 8A and B, p53 translocated into the cytoplasm. The colocalization of MRPL41 and p53 was also confirmed via confocal microscopy (Fig. 8C).

MRPL41 induces expression of p53 and $p27^{Kip1}$ in growth-inhibitory conditions. A previous study has demonstrated that ribosomal protein L11 mediates actinomycin D- or serum starvation-induced p53 activation (1). We used RNAi to inhibit MRPL41 expression. Transient transfection of MRPL41 RNAi into MRPL41-overexpresing H211 cells efficiently down-regu-

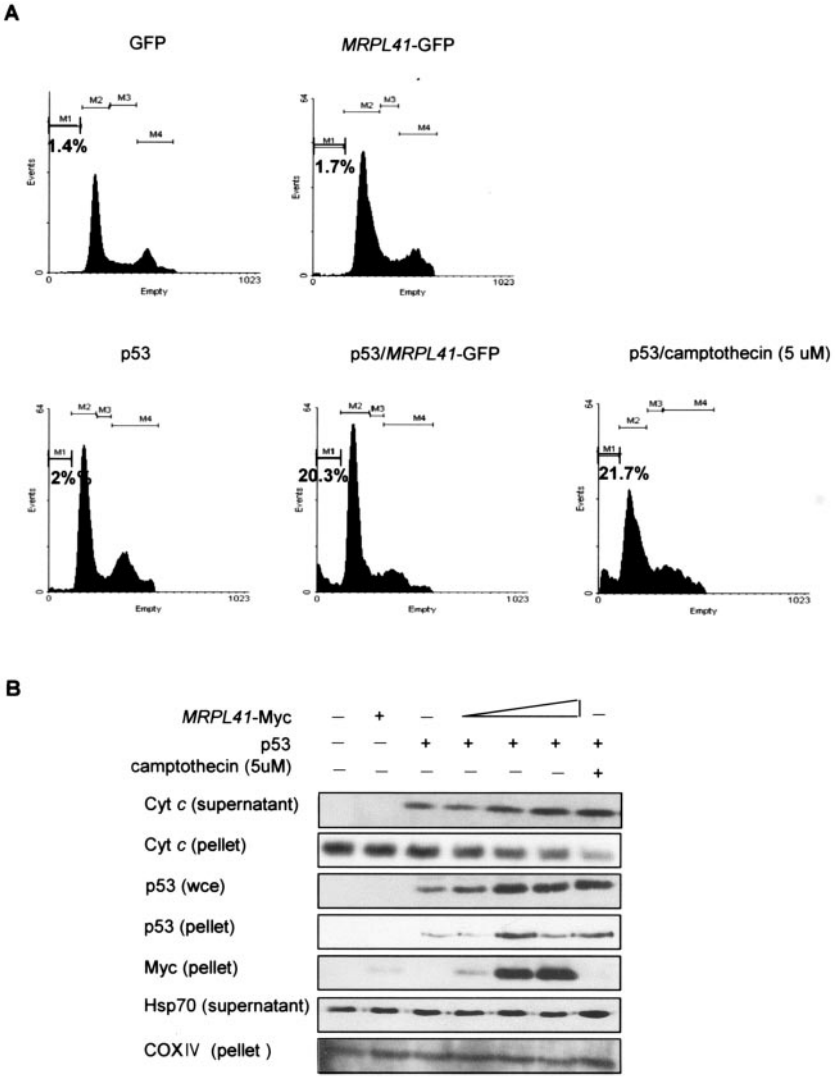

FIG. 7. MRPL41 induced p53-dependent apoptosis. (A) Effects of MRPL41 on p53-mediated apoptosis in H1299 cells. p53, GFP, and *MRPL41*-GFP were transfected into H1299 cells as indicated. Twenty-four hours after transfection, cells were stained with propidium iodide, and the DNA content of GFP-expressing cells was quantitated. Over 5,000 cells were used in this analysis. As a positive control, p53 was transfected into H1299 cells. Twenty-four hours after transfection, cells were treated with 5 μM camptothecin for 6 h. (B) MRPL41 induces cytochrome *c* release in cells cotransfected with p53 and MRPL41. H1299 cells cotransfected with equal amounts of p53 and increasing amounts of *MRPL41*-Myc (0.1 μg, 0.3 μg, and 0.5 μg), and mitochondrial (pellet) and cytosolic fractions (supernatant) were prepared from transfected cells. Ten micrograms of fraction was loaded, and Western blot analysis of cytochrome *c*, p53, COXIV, and PCNA was performed. wce, whole-cell extract.

lated MRPL41 expression (Fig. 9A). To determine the biological functions of MRPL41, HEK 293 and H211 cells were treated with actinomycin D or serum starved. Even though actinomycin D or serum starvation could not induce expression of MRPL41, both enhanced the amounts of p53 and $p27^{Kip1}$. Serum starvation also induced expression of p53 and $p27^{Kip1}$ (Fig. 9B). To observe whether MRPL41 mediates actinomycin D-induced p53 and $p27^{Kip1}$ stabilization, HEK 293 and H211 cells were treated with MRPL41 RNAi to inhibit expression of MRPL41. As shown in Fig. 9C, actinomycin D treatment failed to induce p53 and $p27^{Kip1}$ in the absence of MRPL41. Overall, these data demonstrate that MRPL41 triggered p53 translocation into the mitochondria by enhancing the stability of p53 in growth-inhibitory conditions.

DISCUSSION

We have identified the MRPL41 protein, which is localized in the mitochondria, stabilizes p53 protein, and enhances its translocation into the mitochondria, thus inducing apoptosis. In the absence of p53, MRPL41 stabilizes $p27^{Kip1}$ and arrests the cell cycle at the G_1 phase. Our results suggest that MRPL41 may contribute to the tumor suppressor activity of p53 in cancer development, possibly by either p53-mediated apoptosis or $p27^{Kip1}$-mediated cell cycle arrest.

p53 plays a key role in apoptosis, growth arrest, and DNA repair, by virtue of its ability to function as a transcription factor. p53-dependent cellular regulation occurs mainly in the nucleus. Recent reports have shown that p53 translocates into

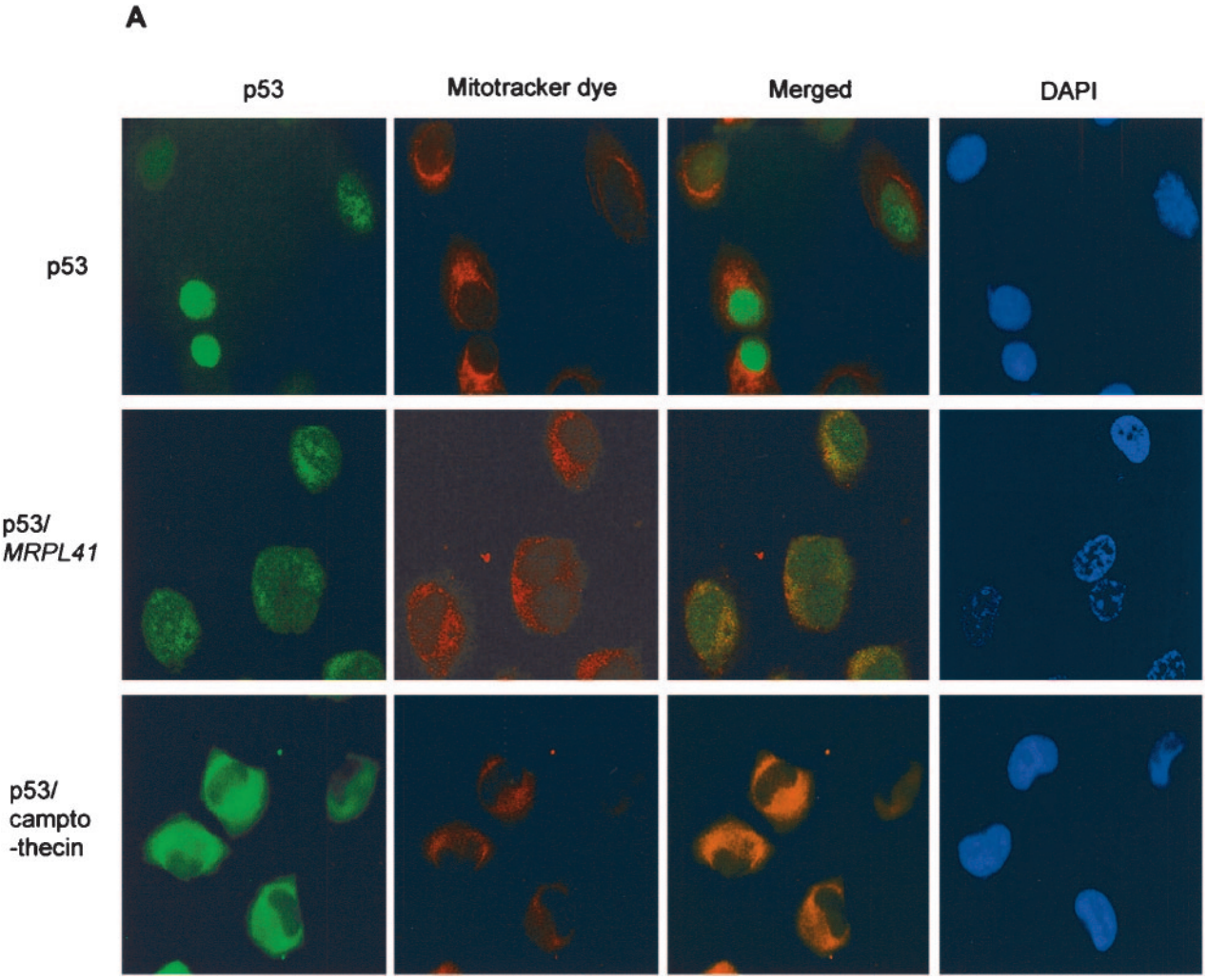

FIG. 8. MRPL41 induced the mitochondrial localization of p53. (A) The translocation of p53 induced by MRPL41. H1299 cells were transfected with either p53 alone or with *MRPL41*-Myc. After 24 h, cells were fixed and stained with anti-p53 antibody (green) in order to visualize the localization of p53. The location of p53 was detected by green fluorescence and was observed under confocal microscopy. Nuclei were stained with DAPI dye. As a positive control, p53 was transfected into H1299 cells. At 24 h after transfection, cells were treated with 5 μM camptothecin for 6 h. (B) H1299 cells were cotransfected with equal amounts of p53 and increasing amounts of *MRPL41*-GFP (0.1 μg, 0.3 μg, 0.5 μg, and 1 μg). Graphs show the percentage of cells exhibiting mitochondrial p53 staining for MRPL41-GFP staining. A total of 300 cells were scored to ascertain the location of p53 under each experimental condition. Data shown represent three independent experiments. (C) The subcellular localization of p53 and MRPL41-GFP was confirmed by confocal microscopy.

the mitochondria after damage, resulting in transcription-independent apoptosis (2, 5, 13, 15, 16, 19). In the mitochondria, p53 interacts with Bcl-2, Bcl-XL, or Bax, thereby inducing the permeabilization of the outer mitochondrial membrane. Previous studies have shown functional differences with regard to the codon 72 polymorphic variants of p53 (5, 16). The Arg72 variant, which exhibited enhanced localization to the mitochondria, was more efficient in terms of inducing apoptosis than was the Pro72 variant. Conversely, the Pro72 variant induced the arrest of the cell cycle at G_1 more efficiently than did the Arg72 variant. The Pro72 variant also induced apoptosis. Our data show that increased *MRPL41* expression results in the enhanced accumulation of p53 and apoptosis in the H1299 cells and triggers p53 translocation into the mitochondria by enhancing the stability of p53, even in the absence of a death stimulus. Although there is no direct evidence to indicate that MRPL41 is involved in p53-dependent apoptosis, it can be assumed that MRPL41 contributes to the increase of p53 stability in response to death stimuli. The molecular mechanisms by which the stability of p53 is enhanced by MRPL41, as well as the mechanisms underlying MRPL41-induced apoptosis, remain to be clarified. One possible explanation is that MRPL41 may block directly or indirectly ubiquitination of p53 and inhibit p53 degradation. The other explanation involves MRPL41 functioning as a proteosome inhibitor and blocking the degradation of p53 and $p27^{Kip1}$, resulting in either apoptosis or cell cycle arrest. However, more will be required in order to elucidate these mechanisms.

Interestingly, even though the NCI-H211 cells expressed p53 at high levels under unstressed conditions, these cells were arrested in the G_1 phase of the cell cycle rather than undergoing apoptosis (Fig. 4). It seems that the p53 present in these

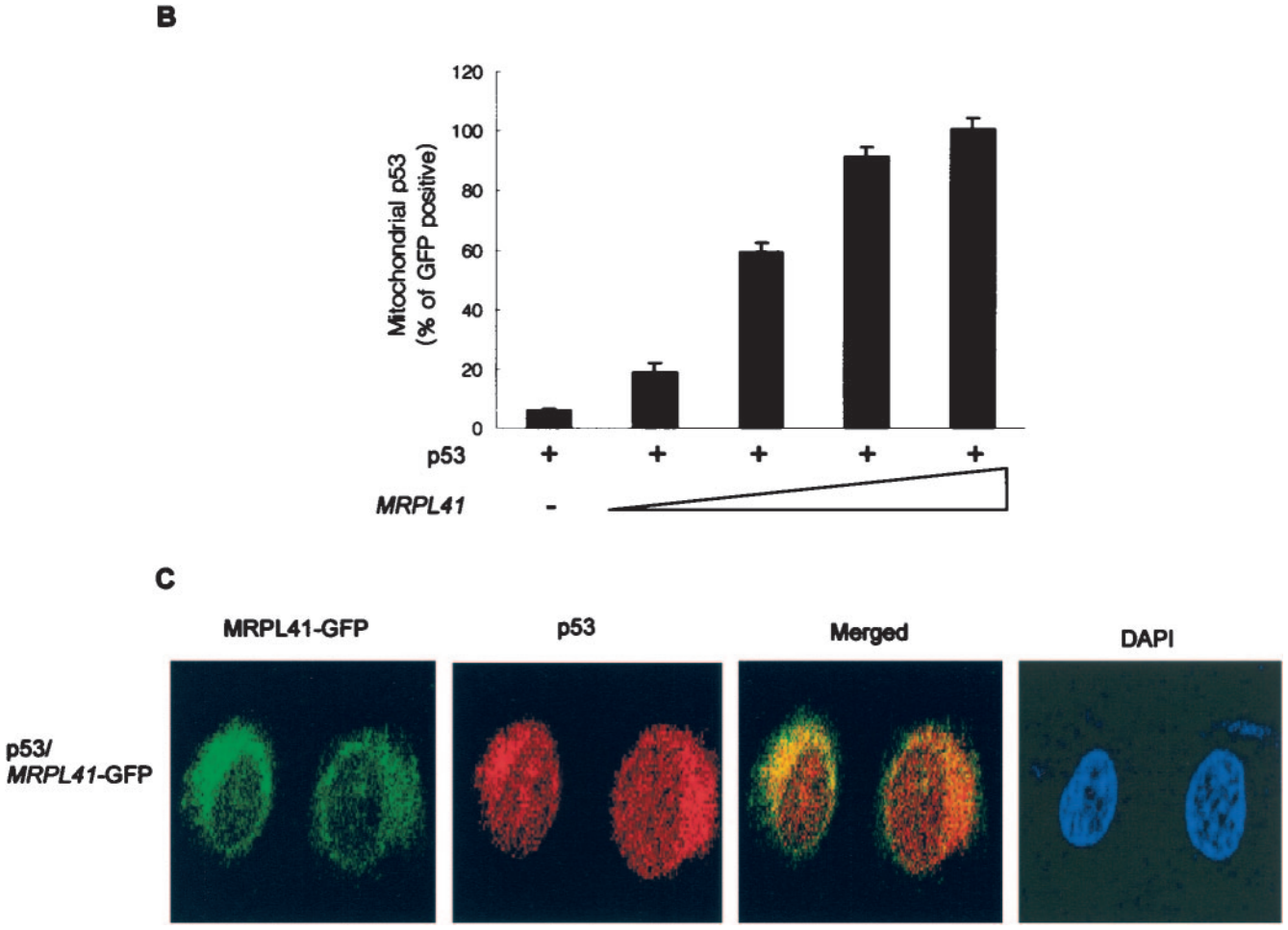

FIG. 8—*Continued*.

cells may be nonfunctional or inactive. The mutant p53 is frequently expressed at much higher levels in unstressed cells. Furthermore, MRPL41 arrested the cell cycle at the G_1 phase in p53-null H1299 cells (Fig. 6F). In the presence of p53, however, MRPL41 induced apoptosis, even under unstressed conditions (Fig. 7). These results demonstrate that MRPL41 plays a role, not only in apoptosis, but also in cell cycle arrest induced by the increased stability of $p27^{Kip1}$.

Although the molecular mechanism controlling the link between ribosomal biogenesis and cell cycle regulation remains obscure, it has recently been reported that three ribosomal proteins, L5, L11, and L23, play important roles in the mediation of growth inhibition by inducing p53-dependent cell cycle arrest (1, 3, 4, 10, 12, 22). These ribosomal proteins interact directly with HDM2. Interaction with HDM2 results in the stabilization and activation of p53, via the prevention of HDM2-mediated p53 ubiquitination and degradation. In this study, we identified mitochondrial ribosomal protein MRPL41, which is encoded by nuclear genes and facilitates protein synthesis within the mitochondria. Our studies demonstrated that MRPL41 employs a distinctly different mechanism from these ribosomal proteins in terms of p53 activation. The three ribosomal proteins L5, L11, and L23 activate p53-dependent cell cycle arrest via interactions with HDM2. However, MRPL41 induces p53-dependent apoptosis by triggering p53 translocation to the mitochondria without interacting with HDM2 or p53, probably through interaction with other apoptotic effectors. We attempted to ascertain whether MRPL41 stabilizes p53 via direct interaction. In service of this goal, we performed an immunoprecipitation assay with polyclonal anti-p53 antibody or monoclonal anti-Myc antibody. On cells stably transfected with *MRPL41*-Myc, p53 and MRPL41-Myc were coprecipitated by either anti-p53 antibody or anti-Myc antibody. No interactions were observed to occur between MRPL41 and p53 or MDM2 (data not shown). These data demonstrated that MRPL41 does not function as a component of the HDM2-p53 pathway in the regulation of cell cycle progression, but rather as a component which mediates the stabilization of p53 in the induction of apoptosis.

In summary, our data demonstrate that MRPL41 increases the accumulation of p53 at the posttranslational level and induces cell cycle arrest at the G_1 phase via the augmentation of $p27^{Kip1}$ expression in the absence of p53. These data suggest that MRPL41 plays a dual role, as either a component in the p53-independent arrest of the cell cycle in the G_1 phase or as a component which induces apoptosis in the presence of p53. We speculate that MRPL41 may contribute to the tumor suppressor activity of p53 in cancer development, possibly via

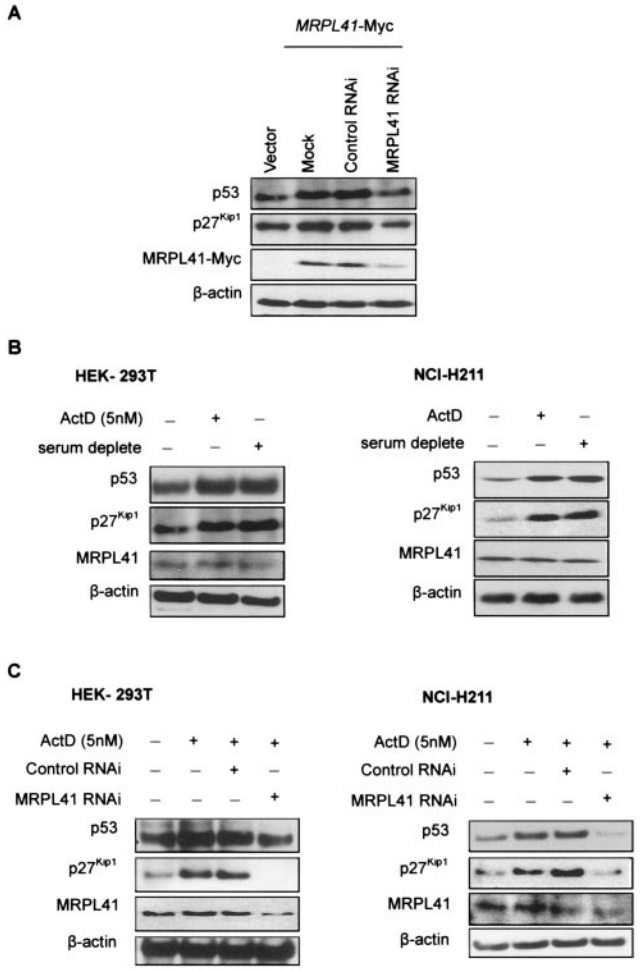

FIG. 9. MRPL41 is essential for p53 and p27 activation on growth-inhibitory conditions. (A) NCI-H211 cells stably expressing MRPL41-Myc were transfected with MRPL41 RNAi or with a control RNA duplex and were harvested 24 h later. Forty micrograms of cell lysates was resolved by SDS-PAGE, and Western blotting with anti-p53, anti-$p27^{Kip1}$, anti-Myc, or anti-β-actin antibodies was performed. (B) HEK-293T and NCI-H211 cells were treated with actinomycin D (5 nM) or serum starved and then harvested 24 h later. Forty micrograms of cell lysates was resolved by SDS-PAGE, and Western blotting with anti-p53, anti-$p27^{Kip1}$, anti-MRPL41, or anti-β-actin antibodies was performed. (C) HEK-293T and NCI-H211 cells were transfected with MRPL41 RNAi or with a control scrambled RNA duplex for 24 h, followed by actinomycin D treatment (5 nM) for an additional 24 h. Forty micrograms of cell lysates was resolved by SDS-PAGE, and Western blotting with anti-p53, anti-$p27^{Kip1}$, anti-MRPL41, or anti-β-actin antibodies was performed.

p53-mediated apoptosis and/or $p27^{Kip1}$-mediated cell cycle arrest and the regulation of cell cycle checkpoints. Further study is required in order to elucidate the mechanism underlying the cellular regulation of MRPL41, as well as the molecular mechanisms by which MRPL41 increases p53 stability and induces cell cycle arrest at the G_1 phase.

ACKNOWLEDGMENTS

This study was supported by a grant of the 2002 Korean National Cancer Control Program, Ministry of Health & Welfare, Republic of Korea; by a grant from the Molecular and Cellular BioDiscovery Research Program (M1-0311-00-0035) of the Ministry of Science and Technology of Korea; and by a grant of the Research Center for Woman's Diseases of the KOSEF.

REFERENCES

1. **Bhat, K. P., K. Itahana, A. Jin, and Y. Zhang**. 2004. Essential role of ribosomal protein L11 in mediating growth inhibition-induced p53 activation. EMBO J. **23:**2402–2412.
2. **Chipuk, J. E., T. Kuwana, L. Bouchier-Hayes, N. M. Droin, D. D. Newmeyer, M. Schuler, and D. R. Green**. 2004. Direct activation of Bax by p53 mediates mitochondrial membrane permeabilization and apoptosis. Science **303:**1010–1014.
3. **Dai, M. S., and H. Lu**. 2004. Inhibition of MDM2-mediated p53 ubiquitination and degradation by ribosomal protein L5. J. Biol. Chem. **279:**44475–44482.
4. **Dai, M. S., S. X. Zeng, Y. Jin, X. X. Sun, L. David, and H. Lu**. 2004. Ribosomal protein L23 activates p53 by inhibiting MDM2 function in response to ribosomal perturbation but not to translation inhibition. Mol. Cell. Biol. **24:**7654–7668.
5. **Dumont, P., J. I. Leu, A. C. Della Pietra III, D. L. George, and M. Murphy**. 2003. The codon 72 polymorphic variants of p53 have markedly different apoptotic potential. Nat. Genet. **33:**357–365.
6. **Giaccia, A. J., and M. B. Kastan**. 1998. The complexity of p53 modulation: emerging patterns from divergent signals. Genes Dev. **12:**2973–2983.
7. **Habuchi, T., J. Devlin, P. A. Elder, and M. A. Knowles**. 1995. Detailed deletion mapping of chromosome 9q in bladder cancer: evidence for two tumour suppressor loci. Oncogene **11:**1671–1674.
8. **Haupt, Y., R. Maya, A. Kazaz, and M. Oren**. 1997. Mdm2 promotes the rapid degradation of p53. Nature **387:**296–299.
9. **Hornigold, N., J. Devlin, A. M. Davies, J. S. Aveyard, T. Habuchi, and M. A. Knowles**. 1999. Mutation of the 9q34 gene *TSC1* in sporadic bladder cancer. Oncogene **18:**2657–2661.
10. **Jin, A., K. Itahana, K. O'Keefe, and Y. Zhang**. 2004. Inhibition of HDM2 and activation of p53 by ribosomal protein L23. Mol. Cell. Biol. **24:**7669–7680.
11. **Levine, A. J**. 1997. p53, the cellular gatekeeper for growth and division. Cell **88:**323–331.
12. **Lohrum, M. A., R. L. Ludwig, M. H. Kubbutat, M. Hanlon, and K. H. Vousden**. 2003. Regulation of HDM2 activity by the ribosomal protein L11. Cancer Cell **3:**577–587.
13. **Marchenko, N. D., A. Zaika, and U. M. Moll**. 2000. Death signal-induced localization of p53 protein to mitochondria. A potential role in apoptotic signaling. J. Biol. Chem. **275:**16202–16212.
14. **Michael, D., and M. Oren**. 2003. The p53-Mdm2 module and the ubiquitin system. Semin. Cancer Biol. **13:**49–58.
15. **Mihara, M., S. Erster, A. Zaika, O. Petrenko, T. Chittenden, P. Pancoska, and U. M. Moll**. 2003. p53 has a direct apoptogenic role at the mitochondria. Mol. Cell **11:**577–590.
16. **Pim, D., and L. Banks**. 2004. p53 polymorphic variants at codon 72 exert different effects on cell cycle progression. Int. J. Cancer **108:**196–199.
17. **Polyak, K., Y. Xia, J. L. Zweier, K. W. Kinzler, and B. Vogelstein**. 1997. A model for p53-induced apoptosis. Nature **389:**300–305.
18. **Ruggero, D., and P. P. Pandolfi**. 2003. Does the ribosome translate cancer? Nat. Rev. Cancer **3:**179–192.
19. **Sansome, C., A. Zaika, N. D. Marchenko, and U. Moll**. 2001. Hypoxia death stimulus induces translocation of p53 protein to mitochondria. Detection by immunofluorescence on whole cells. FEBS Lett. **488:**110–115.
20. **Suzuki, K., T. Ogura, T. Yokose, K. Nagai, K. Mukai, T. Kodama, Y. Nishiwaki, and H. Esumi**. 1998. Loss of heterozygosity in the tuberous sclerosis gene associated regions in adenocarcinoma of the lung accompanied by multiple atypical adenomatous hyperplasia. Int. J. Cancer **79:**384–389.
21. **Takamochi, K., T. Ogura, K. Suzuki, H. Kawasaki, Y. Kurashima, T. Yokose, A.Ochiai, K. Nagai, Y. Nishiwaki, and H. Esumi**. 2001. Loss of heterozygosity on chromosomes 9q and 16p in atypical adenomatous hyperplasia concomitant with adenocarcinoma of the lung. Am. J. Pathol. **159:**1941–1948.
22. **Zhang, Y., G. W. Wolf, K. Bhat, A. Jin, T. Allio, W. A. Burkhart, and Y. Xiong**. 2003. Ribosomal protein L11 negatively regulates oncoprotein MDM2 and mediates a p53-dependent ribosomal-stress checkpoint pathway. Mol. Cell. Biol. **23:**8902–8912.
23. **Zhao, K. N., L. Tomlinson, W. J. Liu, W. Gu, and I. H. Frazer**. 2003. Effects of additional sequences directly downstream from the AUG on the expression of GFP gene. Biochim. Biophys. Acta **1630:**84–95.